Journal of Crystal Growth 524 (2019) 125157

Contents lists available at ScienceDirect

Journal of Crystal Growth

journal homepage: www.elsevier.com/locate/jcrysgro

Magnetic properties of high-pressure optical floating-zone grown $LaNiO_3$ single crystals

Kaustav Dey[a,*], Waldemar Hergett[a], Prachi Telang[b], Mahmoud M. Abdel-Hafiez[a,c], Rüdiger Klingeler[a,d]

[a] Kirchhoff Institute for Physics, Heidelberg University, 69120 Heidelberg, Germany
[b] Department of Physics, Indian Institute of Science Education and Research, Pune, Maharashtra 411008, India
[c] Harvard University, Cambridge, MA 02138, USA
[d] Centre for Advanced Materials (CAM), Heidelberg University, 69120 Heidelberg, Germany

ARTICLE INFO

Communicated by Pierre Muller

Keywords:
A1. Characterization
A2. High-pressure optical floating zone technique
A2. Single crystal growth
B1. Perovskite nickelate
B2. Magnetic materials

ABSTRACT

Macroscopic cm-sized single crystals of distorted perovskite $LaNiO_3$ have been grown by means of the optical floating-zone method at oxygen pressures of 40 and 80 bar, respectively. Depending on the growth parameters, the crystals feature a transition to long-range antiferromagnetic order as indicated by magnetic susceptibility and specific heat studies or lack of magnetic order. Our findings resemble recent contradictory reports which either imply the presence of unexpected antiferromagnetism (Guo et al., 2018) or the absence of magnetic order (Zhang et al., 2017; Wang et al., 2018). Our data indicate that long-range magnetic order is not intrinsic to $LaNiO_3$.

1. Introduction

Rare earth nickelate perovskites $RNiO_3$ (R = Pr-Lu, Y) are an extensively studied class of compounds, exhibiting band-width controlled metal-insulator (MI) transition as a function of temperature that varies with the rare-earth size [4,5]. Apart from $LaNiO_3$, which exhibits Pauli paramagnetism, all $RNiO_3$ compounds show MI transition with antiferromagnetic ground state [5]. However, for nearly three decades intense research on bulk $RNiO_3$ compounds has been restricted to polycrystalline samples only as single-crystals had not been accessible due to necessity of high temperature and pressure to keep nickel in the unusual +3 valence state [6,7]. Recent technological advances in the field of crystal growth enable growth of high-quality single crystals of previously non-accessible systems, e.g., by applying high pressure [8–17]. In fact, single crystals of $LaNiO_3$ were grown recently, for the first time, using the high-pressure optical floating zone furnace employing pressures as high as 150 bar [1,2]. Subsequent magnetic studies on $LaNiO_3$ single crystals revealed a markedly different behaviour [1,2] as compared to the polycrystalline $LaNiO_3$ samples [18–20]. Contradictory reports on the magnetic ground state of $LaNiO_3$ have been published recently. Guo et al. by means of magnetisation, specific heat and neutron diffraction experiments on $LaNiO_3$ single crystals report an antiferromagnetic metallic ground state [1] whereas no long range order was observed by Zhang et al. [2]. Recent DFT calculations [21] find the *Pnma* structure to be marginally favoured compared to the experimentally reported $R\bar{3}c$ structure and antiferromagnetic order could be stabilized in both phases. It is important to re-investigate the intrinsic nature of magnetism in $LaNiO_3$, as it could provide important clues towards understanding the driving mechanism responsible for the MI transition in the $RNiO_3$ perovskite nickelates.

In the present work, we report the successful growth of $LaNiO_3$ single crystals by the high O_2-pressure optical floating-zone technique. Laue analysis implies the presence of macroscopic single crystalline grains and phase purity is confirmed by means of room temperature X-ray diffraction. The static magnetic susceptibility $\chi = M/B$ vs. temperature of $LaNiO_3$ single crystals grown under 40 bar and 80 bar is reported. Crystals extracted from areas well separated from the molten zone regions display magnetic susceptibilities in accordance with Zhang et al.[2]. In particular, the crystals do not exhibit anomalies as observed by Guo et al. [1]. In contrast, single crystals extracted nearby the molten zone region exhibit kinks in χ at around 155 K and corresponding jumps in the specific heat. Based on magnetisation and specific heat measurements on our $LaNiO_3$ single crystals, we conclude that long range ordering in $LaNiO_3$ may not be intrinsic and that the effect of oxygen deficient phases, i.e, $LaNiO_{3-\delta}$ needs to be considered seriously when interpreting the physical properties of $LaNiO_3$.

* Corresponding author.
E-mail address: kaustav.dey@kip.uni-heidelberg.de (K. Dey).

https://doi.org/10.1016/j.jcrysgro.2019.125157
Received 14 March 2019; Received in revised form 5 July 2019; Accepted 17 July 2019
Available online 28 July 2019

2. Experimental details

Precursors for the crystal growth were prepared via standard solid state reaction method. La_2O_3 was calcined overnight at 900 °C to remove absorbed water. Stoichiometric amounts of La_2O_3 and NiO were thoroughly ground in an agate mortar and the resulting mixture was sintered at 1000 °C for 24 h in O_2 flow of 250 sccm. The obtained powder was re-ground, densely packed in a rubber tube and isostatically pressed at 60 MPa to obtain cylindrical shaped rods of 6–8 cm in length and 5 mm in diameter. These rods were sintered at 1150 °C in air for several days and used as feed and seed rods. The crystal growth was carried out in a high-pressure optical floating-zone (FZ) furnace (HKZ, SciDre) [9]. A Xenon arc lamp operating at 3.5 kW was employed and the growth was performed inside a sapphire chamber of 72 mm in length and 20 mm wall thickness. All the growth experiments were performed in O_2 atmosphere at elevated pressures of 40 and 80 bar, maintaining an O_2 flow rate of 0.1 l/min. The feed and seed rods were counter rotated at 10 rpm for homogeneous mixing and thermal stability of the zone. The feed rod was pulled at 7 mm/h and the seed rod was pulled at about 4–6 mm/h to ensure enough liquid volume in the zone and to maintain the zone stability. *In-situ* temperature profiles of the sample and molten zone were obtained stroboscopically by means of a two-color pyrometer which can be moved vertically along the growth chamber during the growth process.

Phase purity was studied by means of X-ray diffraction (XRD) measurements on a Bruker D8 Advance ECO diffractometer with Cu Kα source. Data have been collected at room temperature in the 2θ range of 10–70 ° with 0.02 ° step-size and integration time of 180 s per step. Rietveld refinement of the obtained patterns was done using the FullProf Suite 2.0 [22]. Oxygen content was determined by thermogravimetry (TGA) using the STA 449 F1 Jupiter by NETZSCH equipped with a WRe type thermocouple. Pulverized samples (≈60 mg) were placed in an alumina crucible and heated at the rate of 10 K/min up to 550 °C with dwell time of two hours at the highest temperature. The measurements were done under reducing Ar-10%/H_2 gas flow at 40 ml/min. Magnetisation was measured using a superconducting quantum interference device (SQUID) magnetometer (Quantum Design MPMS-XL5). Specific heat measurements were carried out in a Quantum Design PPMS using the relaxation method.

3. Results and discussions

The crystal growth was carried out successfully by maintaining a stable zone in the presence of an elevated O_2 pressure between 40 and 80 bar. Elevated pressure is required to obtain phase pure $LaNiO_3$ single crystals which contains Ni in unusual +3 oxidation state [2]. Simple solid state reaction of the precursors at high temperatures ($T > 800$ °C) and ambient pressure leads to the formation of other oxide phases (Ruddlesden-Popper) containing Ni in its usual +2 state [23]. One of challenges we faced in the high-pressure optical growth of $LaNiO_3$ is the cracking of the feed and seed rods during the growth. The density of the cracks formed during 80 bar growth is higher than at 40 bar. We attribute this to the fact that increasing the gas pressure leads to a sharper temperature gradient along the rod facilitating the crack formation [24]. The larger number of cracks at 80 bar made it difficult to form and maintain a stable zone, sometimes leading to the breaking and falling of the feed rod. To avoid the cracking issue, highly dense feed rods have been made. Sintering the rods at a higher temperature, i.e., at 1150 °C, with longer dwelling time of about 4–6 days was found suitable to completely overcome cracking. During the growth, the feeding rate is kept higher than the crystal pulling rate to maintain a stable zone leading to the formation of broad crystals of about 5–6 mm in diameter. The length of the longest as-grown single crystal rod obtained in our experiment at 40 bar O_2 pressure is about 1.4 cm as shown in Fig. 2.

Fig. 1 shows the floating-zone formed during the growth along with the respective temperature profile of the sample and the molten region.

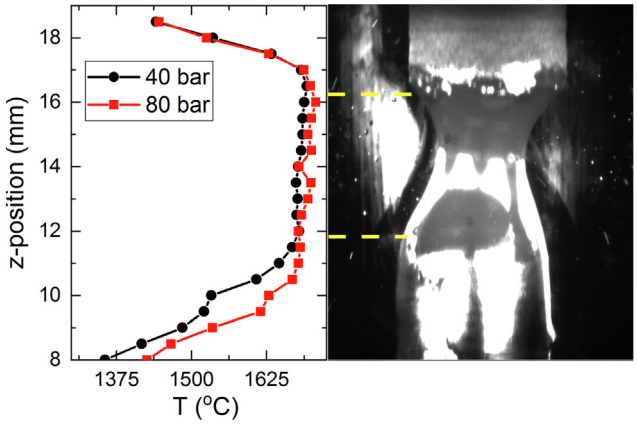

Fig. 1. Vertical in situ temperature profile of the sample at and around the melting zone during the growth as measured by the pyrometer (left) and real-time image of a typical $LaNiO_3$ floating zone (right).

The profile demonstrates a plateau-like shape showing a broad central region corresponding to the melt. The temperature of the liquid floating-zone amounts to 1681 ± 5 °C at 40 bar and 1696 ± 8 °C at 80 bar O_2 pressure, respectively. The near vertical profile in the temperature of the floating-zone indicates that the zone-temperature is near constant. This indicates that counter rotation of feed and seed rods at 10 rpm is appropriate to achieve a homogeneous temperature distribution in the floating-zone. The resulting as-grown $LaNiO_3$ boule is shown in Fig. 2. Laue diffraction performed at several spots along the length of the boule to detect single-crystalline grains confirms cm-size single-crystalline grains in the obtained samples with good crystallinity.

To study the phase purity of the grown single crystals, powder XRD was performed on several crushed and pulverized single crystalline pieces cut along the length of the grown rods. Fig. 3 shows Rietveld refinements of the obtained XRD patterns for the growths performed at 40 and 80 bar, respectively. The results imply that our single crystals exhibit the $R\bar{3}c$ space group and confirm phase purity within the accuracy of the powder XRD measurements. The lattice parameters obtained from Rietveld analysis of the room temperature XRD patterns is listed in Table 1. Note that the Ni-O-Ni bond angle is less than 180 ° indicating that $LaNiO_3$ has a distorted perovskite structure. The oxygen content of the $LaNiO_3$ crystals grown under 40 bar was determined to be 2.976(1) by TGA measurements which implies $\delta \approx -0.023(8)$ vacancies per formula unit. For the samples grown at 80 bar the oxygen content amounts to 2.979(1), i.e. $\delta \approx -0.020(9)$. Note that the oxygen deficiency is in a similar range as reported by Zhang et al. [2]. In contrast, the crystals extracted close to the molten floating zone (LNO40.1) exhibit a significantly larger oxygen deficiency of $\delta \approx -0.183(8)$ vacancies per formula unit resulting in an oxygen content of 2.816(9). As noted in Table 1, the Ni—O—Ni bond angle as well as the lattice parameters increase with increase in oxygen vacancies but no change is observed in the crystal structure symmetry from XRD measurements on the most oxygen deficient samples.

Fig. 4 shows the static magnetic susceptibility $\chi = M/B$ vs. T for several $LaNiO_3$ single crystals grown under 40 and 80 bar, respectively.

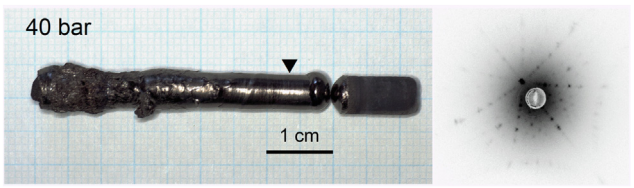

Fig. 2. As-grown boule of $LaNiO_3$ grown at 40 bar O_2-pressure and representative back-scattered Laue pattern taken along the growth direction at the position marked by the black triangle.

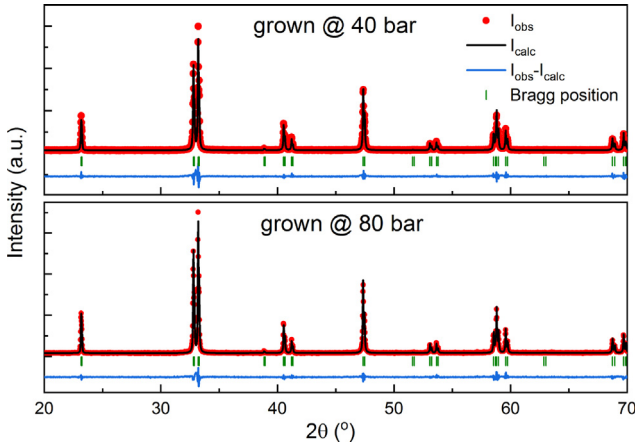

Fig. 3. Room temperature XRD-patterns and corresponding Rietveld refinements of powdered $LaNiO_3$ single crystals grown at 40 and 80 bar O_2 pressure, respectively. The observed diffraction patterns are shown in red, calculated patterns in black, and the difference between the observed and calculated patterns is shown in blue. Vertical green ticks denote the allowed Bragg positions.The R parameters of the fits are $R_{wp} = 15.5$, $R_e = 8.85$, $\chi^2 = 3.05$ for 40 bar and $R_{wp} = 14$, $R_e = 9.42$, $\chi^2 = 2.21$ for 80 bar respectively. (For interpretation of the references to colour in this figure legend, the reader is referred to the web version of this article.)

Table 1
Lattice constants, Ni—O—Ni bond angle of $R\bar{3}c$-$LaNiO_3$ as determined from Rietveld analysis of room temperature X-ray diffraction data, and oxygen vacancy content δ. Samples marked as LNO40 and LNO80 are taken from two different boules grown at 40 and 80 bar, respectively. $*$ mark indicates a sample extracted close to the solidified floating-zone (about 2 mm away) which exhibits anomalies in the susceptibility and specific heat data (cf. Figs. 4 and 5). All other crystals are extracted far from the solidified zone and exhibit no such anomalies. Refer the text for further information.

Sample	a (Å)	c (Å)	∢ Ni—O—Ni (°)	δ
LNO40.1*	5.459(2)	13.136(2)	169.9	−0.183(8)
LNO40.2	5.457(3)	13.130(4)	165.3(7)	−0.023(8)
LNO80.1	5.457(2)	13.130(1)	164.8(3)	−0.020(9)
LNO80.2	5.457(6)	13.129(7)	164.8(3)	–

The overall behaviour $\chi(T)$ is consistent with previous reports on single crystals by Zhang et al. [2] and Guo et al. [1], but markedly differ from the magnetic susceptibility of polycrystalline $LaNiO_3$[18,20] (refer to the digitized data in Fig. 4). While χ is of the same order of magnitude, it demonstrates only very weak temperature dependence in polycrystals and is quantitatively well described by the sum of Pauli paramagnetism and a Curie contribution. Instead, the data in Fig. 4 shows a broad maximum in addition to the Curie-like upturn at low temperatures which may be associated to quasi-free magnetic impurities, e.g., due to the presence of Ni^{2+} in the $\lesssim 1\%$ range [2,19]. A smaller upturn in susceptibility, as observed (Fig. 4) in the crystals grown under 80 bar to that of 40 bar implies less quasi-free moments suggesting that higher pressure reduces the presence of Ni^{2+} defects in the grown $LaNiO_3$ single crystals.

Detailed inspection of the magnetic susceptibility in the region of the maximum exhibits no anomalies for crystals grown at 40 and 80 bar (see Fig. 4). The susceptibility results are in accordance with Zhang et al. Surprisingly, the single crystalline pieces extracted nearer, i.e., about 2 mm away from the solidified zone of one of the boules (LNO40.1) and which possess the highest oxygen deficiency as obtained from the TGA data, exhibit a kink in χ at $T_N = 151$ K (see Fig. 4). In fact, several pieces extracted from a region close to the solidified floating-zone exhibit similar anomalies at temperatures 151–157 K as shown in Fig. 4. The corresponding specific heat data for one of these single

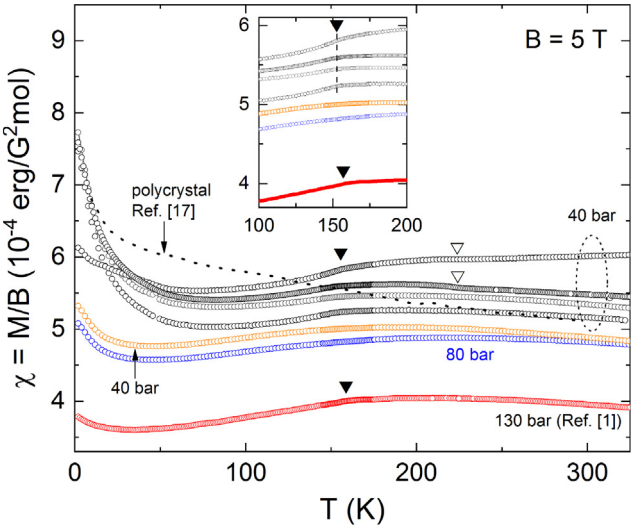

Fig. 4. Temperature dependence of the static magnetic susceptibility $\chi = M/B$ of several $LaNiO_3$ single crystals grown under 40 and 80 bar O_2 pressure, respectively, at $B = 5$ T. The inset shows χ in the temperature range $100\,K \leqslant T \leqslant 200$ K, i.e., highlighting the regime where some of the samples evolve antiferromagnetic order. Anomalies signaling the evolution of antiferromagnetism are marked by filled triangles. Open triangles mark anomalies indicative of a ferromagnetic impurity phase (see the text).

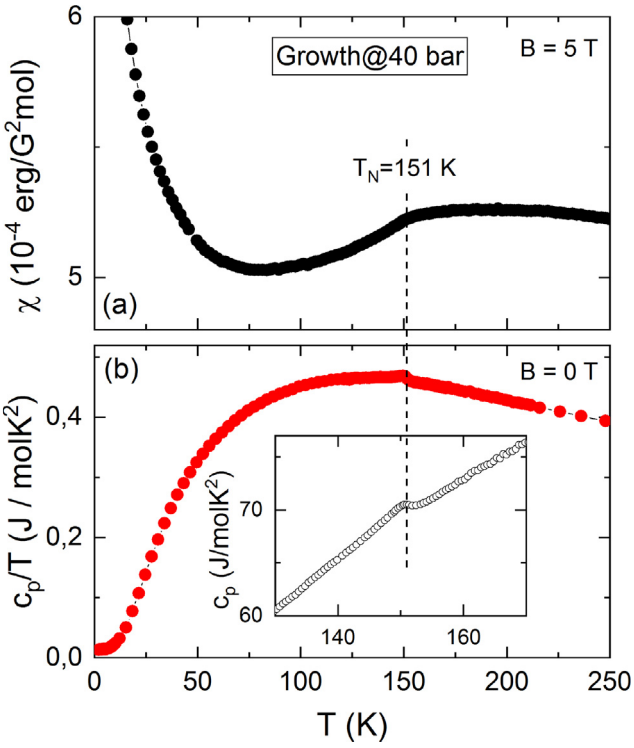

Fig. 5. Temperature dependence of (a) magnetic susceptibility and (b) heat capacity of a $LaNiO_3$ single crystal grown under 40 bar of O_2 pressure.

crystalline pieces (Fig. 5b) show a small jump Δc_p at T_N which is usually indicative of the onset of long-range order. Note that the observed anomalies are in the same temperature range as previously reported by Guo et al. [1] where anomalies in the susceptibility and the specific heat were observed at 157 K (see the digitized data in Fig. 4). Quarter integer peaks in single crystal neutron diffraction enabled them to conclude the presence of long-range antiferromagnetic order. These findings challenged all previous studies where $LaNiO_3$ was reported to

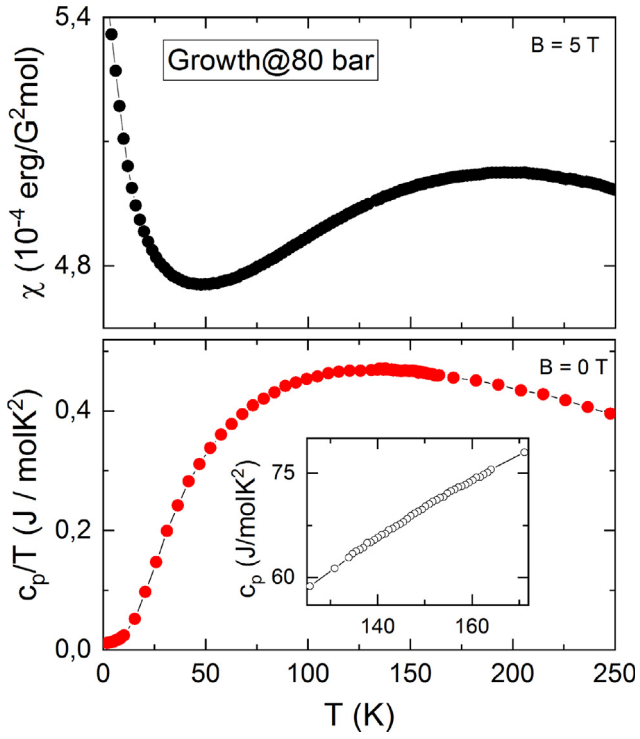

Fig. 6. Temperature dependence of (a) magnetic susceptibility and (b) heat capacity of a $LaNiO_3$ single crystal grown under 80 bar of O_2 pressure.

be a Pauli paramagnetic metal. As shown in Figs. 4 and 5, we observe similar anomalies in χ and c_p only for the single crystals extracted very close to the solidified zones. The specific heat data for a single crystalline piece grown at 80 bar pressure (i.e. LNO80.1 and LNO80.2) and taken far away from the zone exhibits no anomaly (see Fig. 6). This indicates an extrinsic nature of the observed anomalies. Note, that the oxygen deficient phases of $LaNiO_3$, i.e., $LaNiO_{3-\delta}$, show various anomalies in magnetic studies depending on δ. For example, $LaNiO_{2.5}$ reportedly shows antiferromagnetism at $T_N = 140$ K [25] whereas $LaNiO_{2.75}$ shows ferromagnetism at $T_C = 230$ K [26]. Indeed, depending on growth conditions of the samples and vicinity to the solidified floating zone, the susceptibility indicates a ferromagnetic impurity phase, presumingly $LaNiO_{2.75}$, as shown by a feature at $T \approx 225$ K (see open triangles in Fig. 4). Comparison of the anomaly with data on $LaNiO_{2.75}$ from Ref. [26] suggests ~5(2)% of this impurity phase in crystals taken from direct vicinity of the molten zone. Notably, Wang et. al. [3] reduced $LaNiO_3$ a single crystal without any anomalies in χ to $LaNiO_{3-\delta}$ which resulted in the appearance of clear features at 150 K (showing antiferromagnetism) as well as at 225 K (showing ferromagnetism). If oxygen deficiency is a parameter governing the presence of antiferromagnetism, details of the growth process and in particular the distance of the crystalline grain under study from the zone will be crucial. We emphasize that all crystals showing the above mentioned anomalies have been taken from a region within 2 mm from the frozen floating-zone of the respective boules which in fact exhibits the largest oxygen deficiency. In contrast, $LaNiO_3$ single crystals taken well away from the frozen floating-zone possess a smaller oxygen deficiency and show the behaviour exemplified by Fig. 6.

4. Conclusions

We have successfully grown macroscopic single crystals of $LaNiO_3$ at oxygen pressures of 40 and 80 bar, respectively. Anomalies in static magnetic susceptibility and heat capacity were observed only in single crystals grown under 40 bar pressure and extracted from a region close to the zone. Our results indicate an extrinsic nature of the observed anomalies, most likely arising due to oxygen deficient phases $LaNiO_{3-\delta}$.

Declaration of Competing Interest

The authors declared that there is no conflict of interest.

Acknowledgments

K.D. acknowledges support by the International Max-Planck School IMPRS-QD. Financial support by the German-Egyptian Research Fund (BMBF GERF IV) through project 01DH17036 and by the Deutsche Forschungsgemeinschaft (DFG) through project KL1824/5 is gratefully acknowledged. The authors thank Dr. Surjeet Singh for support and valuable discussions. The authors thank Ilse Glass for technical support. Valuable discussions with Natalija van Well are gratefully acknowledged.

Appendix A. Supplementary material

Supplementary data associated with this article can be found, in the online version, at https://doi.org/10.1016/j.jcrysgro.2019.125157.

References

[1] H. Guo, Z.W. Li, L. Zhao, Z. Hu, C.F. Chang, C.Y. Kuo, W. Schmidt, A. Piovano, T.W. Pi, O. Sobolev, D.I. Khomskii, L.H. Tjeng, A.C. Komarek, Nat. Commun. 9 (1) (2018) 43.
[2] J. Zhang, H. Zheng, Y. Ren, J.F. Mitchell, Cryst. Growth Des. 17 (5) (2017) 2730–2735.
[3] B.-X. Wang, S. Rosenkranz, X. Rui, J. Zhang, F. Ye, H. Zheng, R.F. Klie, J.F. Mitchell, D. Phelan, Phys. Rev. Mat. 2 (6) (2018).
[4] M.L. Medarde, J. Phys. Condens. Matt. 9 (8) (1997) 1679–1707.
[5] G. Catalan, Phase Trans. 81 (7–8) (2008) 729–749.
[6] J.A. Alonso, M.J. Martínez-Lope, M.T. Casais, J.L. García-Muñoz, M.T. Fernández-Díaz, Phys. Rev. B 61 (2000) 1756–1763.
[7] P. Lacorre, J. Torrance, J. Pannetier, A. Nazzal, P. Wang, T. Huang, J. Sol. State Chem. 91 (2) (1991) 225–237.
[8] C. Neef, H. Wadepohl, H.-P. Meyer, R. Klingeler, J. Cryst. Growth 462 (2017) 50–59.
[9] N. Wizent, G. Behr, W. Löser, B. Büchner, R. Klingeler, J. Cryst. Growth 318 (1) (2011) 995–999.
[10] D. Souptel, W. Löser, G. Behr, J. Cryst. Growth 300 (2) (2007) 538–550.
[11] J. Zhang, H. Zheng, C.D. Malliakas, J.M. Allred, Y. Ren, Q. Li, T.-H. Han, J. Mitchell, Chem. Mater. 26 (24) (2014) 7172–7182.
[12] H.B. Cao, Z.Y. Zhao, M. Lee, E.S. Choi, M.A. McGuire, B.C. Sales, H.D. Zhou, J.-Q. Yan, D.G. Mandrus, APL Mater. 3 (6) (2015) 062512.
[13] W.A. Phelan, J. Zahn, Z. Kennedy, T.M. McQueen, J. Sol. State Chem. 270 (2019) 705–709.
[14] H. Guo, Z. Hu, T.-W. Pi, L.H. Tjeng, A.C. Komarek, Crystals 6 (8) (2016).
[15] N. Wizent, N. Leps, G. Behr, R. Klingeler, B. Büchner, W. Löser, J. Cryst. Growth 401 (2014) 596–600.
[16] W. Hergett, C. Neef, H. Wadepohl, H.P. Meyer, M.M. Abdel-Hafiez, C. Ritter, E. Thauer, R. Klingeler, J. Cryst. Growth 515 (2019) 37–43.
[17] N. Wizent, G. Behr, F. Lipps, I. Hellmann, R. Klingeler, V. Kataev, W. Löser, N. Sato, B. Büchner, J. Cryst. Growth 311 (5) (2009) 1273–1277.
[18] K. Sreedhar, J.M. Honig, M. Darwin, M. McElfresh, P.M. Shand, J. Xu, B.C. Crooker, J. Spalek, Phy. Rev. B 46 (10) (1992) 6382–6386.
[19] X.Q. Xu, J.L. Peng, Z.Y. Li, H.L. Ju, R.L. Greene, Phys. Rev. B 48 (2) (1993) 1112–1118.
[20] J.S. Zhou, L.G. Marshall, J.B. Goodenough, Phys. Rev. B 89 (24) (2014).
[21] A. Subedi, SciPost Phys. 5 (2018) 20.
[22] J. Rodríguez-Carvajal, Phys. B: Condens. Matt. 192 (1) (1993) 55–69.
[23] G. Li, J. Yang, Y. Fan, S. Tian, C. Zheng, J. Sol. State Chem. 141 (2) (1998) 457–461.
[24] S. Koohpayeh, D. Fort, J. Abell, Prog. Cryst. Growth Character. Mater. 54 (3) (2008) 121–137.
[25] T. Moriga, O. Usaka, T. Imamura, I. Nakabayashi, I. Matsubara, T. Kinouchi, S. Kikkawa, F. Kanamaru, Bull. Chem. Soc. Japan 67 (3) (1994) 687–693.
[26] R.D. Sánchez, M.T. Causa, A. Caneiro, A. Butera, M. Vallet-Regí, M.J. Sayagués, J. González-Calbet, F. García-Sanz, J. Rivas, Phys. Rev. B 54 (1996) 16574–16578.